NMR spectroscopy of rotating superfluid ^{3}He (Soviet-Finnish Project ROTA Research)

Yu. M. Bun'kov, G. E. Gurgenishvili, M. Kruzius, and G. A. Kharadze

Institute of Physical Problems, Academy of Sciences of the USSR; Institute of Physics of the Academy of Sciences of the Georgian SSR; Low Temperature Laboratory, Helsinki Technical University

Usp. Fiz. Nauk **144**, 141–168 (September 1984)

Experimental and theoretical studies of the properties of superfluid phases of rotating liquid ^{3}He are reviewed. The observational data on nonsingular vortex textures in the rotating A phase as well as experiments revealing a structural transition inside the cores of vortices in the A phase are discussed. The gyromagnetic effect in the rotating B phase, due to the spontaneous magnetization of the vortex cores, is described

1. INTRODUCTION

The beginning of the second decade of research on superfluid liquid ^{3}He was marked by a number of new achievements, linked directly to the study of the properties of the A and B phases in a rotating state. These experiments, performed within the framework of the Soviet-Finnish Project ROTA, made it possible to study in greater depth the nature of the ordering in superfluid ^{3}He and to penetrate to distances of the order of the coherence length, revealing a number of features of the internal structure of the vortices formed in the rotating vessel.

The outstanding results obtained along these lines include the observation of nonsingular vortex textures in rotating ^{3}He-A. The observation of a structural transformation inside the core of the vortex in ^{3}He-B and the observation of a gyromagnetic effect in rotating ^{3}He–B, which appears due to the spontaneous magnetic moment of the vortex concentrated near the core. In this paper the main results of studies of the properties of rotating superfluid phases of ^{3}He are reviewed.

If a vessel with an ordinary viscous liquid is put into uniform rotation, then an equilibrium state corresponding to rigid-body rotation of the liquid with a velocity distribution

$$\mathbf{v}(\mathbf{r}) = \Omega \times \mathbf{r}, \tag{1}$$

where Ω is the angular velocity vector, is quickly established. Such a state can be realized because in a classical liquid there are no obstacles to the formation of local vortical motions with $\nabla \times \mathbf{v} \neq 0$, while the velocity field (1) with

$$\nabla \times \mathbf{v} = 2\Omega \tag{2}$$

ensures that the liquid will be in equilibrium relative to the rotating vessel.

The situation changes radically for an ordered liquid such as superfluid ^{4}He-II. It is well known that the properties of this liquid are described by the macroscopic wave function $\psi = |\psi| e^{i\Phi}$, in addition, coherent (nondissipative) mass transport is characterized by the superfluid velocity.

$$\mathbf{v}_s = \frac{\hbar}{m_4} \nabla \Phi. \tag{3}$$

Since because of (3) $\nabla \times \mathbf{v}_s \equiv 0$, it is clear that the superfluid component cannot be entrained into vortical motion and is therefore incapable of purely rigid-body rotation together with the rotating vessel. Thus the superfluid component[1] ^{4}He-II must attain equilibrium with the rotating vessel via a very unusual (from the point of view of a classical liquid) mechanism, compatible with the requirement that $\nabla \times \mathbf{vs}$ vanish everywhere, except possibly on special lines along which the vorticity is infinite (while the density of the suyperfluid component equals zero). An analysis of this peculiar situation led to the development of a picture according to which equilibrium rotation of ^{4}He-II occurs due to the presence of a system of singular filaments (Onsager-Feynman vortices) that permeate the superfluid liquid along the axis of rotation. In addition, the vortical filaments, which carry the localized vorticity, rotate together with the vessel, whereas the superfluid component undergoes potential (irrotational) flow around the individual vortices. An important fact is that because of (3) the circulation of the superfluid velocity around a closed contour is quantized (in units of h/m_4) and each Onsager-Feynman vortex carries a single quantum of circulation. The vortex structure in rotating ^{4}He-II described above forms against a background of purely rigid-body motion of the normal component with a velocity of $\mathbf{v}_n = \Omega \times \mathbf{r}$.

As is well known,[1] studies of rotating ^{4}He-II, performed over a period of many years, have led to a number of impor-

 0038-5670/84/090731-17$01.80 © 1985 American Institute of Physics

tant results, which have made an important contribution to the physics of the superfluid state of matter. Very recently, quantized vortices in ^{4}He-II were photogaphed (and filmed) and Planck's constant was measured (from the distance between vortices).[2]

The example of ^{4}He-II demonstrates that the ordered (superfluid) liquid undergoes very exotic rotational motion. Amongst the other, presently known, ordered states of matter, the superfluid phases of the light isotope of helium, discoverd in 1971, are undoubtedly of special interest.[3] At temperatures of the order of mK the neutral quantum system-liquid ^{3}He-transforms into a coherent state, which simultaneously exhibits the characteristic features of a superfluid medium, an antiferromagnetic body, and a liquid crystal.

Until very recently, all experimental studies of the properties of the superfluid phases of liquid ^{3}He were conducted in stationary vessels. It is clear, however, that the question of how these ordered phases are entrained into a rotational state is of fundamental significance. The experimental study of this problem encountered great technical difficulties. These difficulties were recently successfully overcome due to the joint efforts of Soviet and Finnish physicists, who developed the unique rotating low-temperature apparatus ROTA, operating in the Low Temperature Laboratory of the Helsinki Technical University in Otaniemi.[4] The first experimental studies of superfluid ^{3}He in a state of rotation were performed using this apparatus within the last two years. A characteristic feature of ^{3}He, which distinguishes it from ^{4}He, is that the properties of the superfluid phases of ^{3}He can be studied by highly sensitive NMR methods. All experimental information obtained thus far on rotating phases of ^{3}He have been obtained from the analysis of NMR spectra. Before reviewing the main results of these studies, we shall give a brief exposition of the basic theoretical prerequisites, based on our current understanding of the nature of superfluid liquid ^{3}He.

2. THEORETICAL PREAMBLE

The transition into the low-temperature ordered state in liquid ^{3}He occurs as a result of the formation (below T_c) of Cooper pairs of quasiparticles. Since at small distances there is a strong repulsion between helium atoms, pairing in a state with angular momentum, $L = 0$ is impossible[5] and effective attraction, which leads to the formation of Cooper pairs, occurs, as has been established, in a state with relative orbital angular momentum $L = 1$. As a result, according to Pauli's principle, Cooper pairs in superfluid ^{3}He must have a total spin $S = 1$, which is confirmed by all available experimental data (see the reviews of Refs. 6–8).

The temperature range from 0.1 mK to 3 mK and the pressure range from 0 bar up to $P_m = 34$ bar (Fig. 1) have now been studied in great detail. The curve of the continuous (second-order) phase transition from the normal state of liquid ^{3}He into the ordered (superfluid) state describes a monotonic growth of the critical temperature $T_c(P)$ with increasing pressure; in addition, at pressures in the range $P < P_0 \approx 21$ bar the B phase is bypassed in the transition into the superfluid phase. As far as the pressure range $P_0 < P < P_m$ is concerned, here, as the temperature is decreased, a transition into the superfluid A phase (whose properties differ markedly from the properties of the B phase) occurs first and the jump-like transition (first-order) into ^{3}He-B occurs only when the temprature is further decreased.

When the macroscopic system transforms into the ordered state, the inherent symmetry of the Hamiltonian is lowered (broken). The superfluid phases of liquid ^{3}He are characterized by the breaking of several types of symmetries, which is what leads to the diversity of their physical properties.

The uniform orbital state of the superfluid A phase is characterized by a macroscopic wave function, which it is convenient to designate with the unit vector $\mathbf{l}$ along which the orbital angular momentum of the Cooper pairs is directed, and the pair of unit vectors $(\mathbf{\Delta}_1, \mathbf{\Delta}_2)$, lying in a plane perpendicular to $\mathbf{l}$ (their orientation in this plane determines the phase of the orbital wave function).

The local orbital state of ^{3}He-A is described by fixing the triad $(\mathbf{\Delta}_1, \mathbf{\Delta}_2, \mathbf{l})$, whose orientation can vary smoothly (on the scale of the coherence length) in space. The variation of the orbital state of the A phase accompanying a displacement by a distance $\delta\mathbf{r}$ is described by a rotation of the triad by the angle

$$\delta\varphi = \mathbf{l}\delta\varphi + \mathbf{l} \times \delta\mathbf{l}, \tag{4}$$

where $\delta\varphi$ describes the rotation around the local orientation of $\mathbf{l}$, while $\delta\mathbf{l}$ describes the change in the orientation of the vector $\mathbf{l}$ itself.

The state determined by the local orientation of the triad $(\mathbf{\Delta}_1, \mathbf{\Delta}_2, \mathbf{l})$ exhibits a loss of symmetry relative to the three-dimensional rotations in the orbital space. It should be noted, however, that the rotation around $\mathbf{l}$, described by the angle $\delta\varphi$, is equivalent to a local change in phase of the wave function by $-\delta\varphi$ and can therefore be compensated by the corresponding gauge transformation $\delta\Phi = \delta\varphi$. Thus the A phase retains the symmetry relative to the combined rotational-gauge transformation mentioned above and only the relative rotational-guage symmetry is broken.

Because of the above-mentioned equivalence of the op-

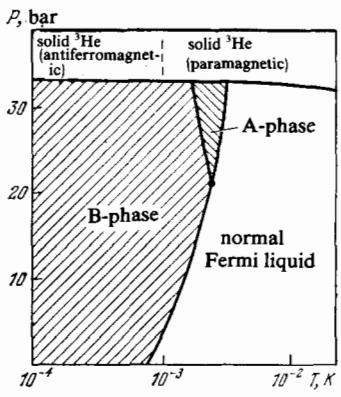

FIG. 1. Phase diagram of ^{3}He near absolute zero (schematically).

eration of rotation around the direction **l** and of the gauge transformation, the Galilean-covariant expression for the superfluid velocity for ^{3}He-A is given by the formula

$$\mathbf{v}_s = -\frac{\hbar}{2m_3}\frac{\delta\varphi}{\delta\mathbf{r}}. \quad (5)$$

Since $\delta\mathbf{\Delta}_2 = \delta\varphi\times\mathbf{\Delta}_2$, we have $\delta\varphi = \mathbf{l}\delta\varphi = -\mathbf{\Delta}_1\delta\mathbf{\Delta}_2$, and it follows from the defintion (5) that for the A phase

$$\mathbf{v}_s = \frac{\hbar}{2m_3}\Delta_{1i}\nabla\Delta_{2i}. \quad (6)$$

We have arrived at the fundamental result that the velocity of coherent mass transport in ^{3}He-A does not reduce to the gradient of the globally determined phase (as occurs in ^{4}He-II). This, of course, associated with the fact that the operation $\delta\varphi = -\mathbf{\Delta}_1\delta\mathbf{\Delta}_2$ is determined only locally and it is impossible to construct with its help in a unique manner the globally determined "phase." Rotational symmetry in spin space is broken in ^{3}He-A, but this symmetry breaking is only partial: a rotation around the direction fixed by the unit vector **d** leaves the state unchanged; in addition, the vector **d** defines the axis along which the projection of the total spin of the Cooper pair equals zero (**Sd** = 0). It is possible to select a local coordinate system relative to which Cooper pairing occurs only in the states with $S_z = \pm 1$, and in the absence of a magnetic field these pairs have equal weights (antiferromagnetic configuration).

Thus under fixed external conditions ^{3}He-A is completely described by the local orientation of the pair of orbital unit vectors $(\mathbf{\Delta}_1, \mathbf{\Delta}_2)$ and the vector **d** (the **l** axis is automatically determined by the relation $\mathbf{l} = \mathbf{\Delta}_1\times\mathbf{\Delta}_2$). If to this we add the fact that the state of the A phase does not change when **d** is replaced by $-\mathbf{d}$ and at the same time the unit vectors $(\mathbf{\Delta}_+, \mathbf{\Delta}_2)$ are rotated by an angle π around the direction **l**, then we obtain a complete description of the internal symmetry of superfluid ^{3}He-A.

All the characteristics listed above can be described by introducing an order parameter for the A phase

$$A_{i\mu} = \frac{\Delta}{\sqrt{2}}(\mathbf{\Delta}_1 + i\mathbf{\Delta}_2)_i\, d_\mu, \quad (7)$$

where $\Delta = \Delta(T)$ determines the amplitude of Cooper pairing.

The superfluid B phase of liquid ^{3}He has a completely different structure. First of all, the gauge symmetry is broken in it. Second, the symmetry under rotation of the spin space relative to the orbital space is lost. This means that under fixed external conditions the ^{3}He-B state is completely described by the local orientation of the axis of the rotation mentioned (defined by the unit vector **n**) and by the angle of rotation θ, as well as by the globally determined phase Φ. Nondissipative mass transport in the B phase is characterized by the superfluid velocity

$$\mathbf{v}_s = \frac{\hbar}{2m_3}\nabla\Phi, \quad (8)$$

as in ^{4}He-II. Everything said above can be summarized by introducing an order parameter for the B phase

$$A_{i\mu} = \frac{\Delta}{\sqrt{3}}R_{i\mu}(\mathbf{n}, \theta)\, e^{i\Phi}, \quad (9)$$

where $R_{i\mu}$ are the components of the matrix of three-dimensional rotations, which realizes rotations of the spin coordinates relative to the orbital coordinates. We note that in the B phase Cooper pairing in spin states with the spin projection along the rotational axis $S_z = \pm 1$ and $S_z = 0$ occurs with equal weights (in the absence of an external magnetic field); in addition, the total angular momentum of the pairs is $\mathbf{J} = 0$.

In the absence of different orienting factors (external fields, superfluid flows, vessel walls) the equilibrium state of the phases of ^{3}He must be spatially uniform. However, under real conditions, due to the orienting influence of the walls of the vessel within which the superfluid liquid is contained in the A phase some spatial distribution (texture) of the orbital axis **l** is established (in order to avoid the breaking of Cooper pairs and loss of the energy of condensation at the boundary with the solid wall, the vector **l** is oriented along the normal to the wall). Taking into account further the fact that the external magnetic field affects the orientation of the vector **d** (the magnetic energy is minimum for $\mathbf{d}\perp\mathbf{H}$), while the spin-orbital forces, due to the weak dipole-dipole interaction between the magnetic moments of ^{3}He nuclei, try to orient **d** along **l**, it becomes obvious that as a result of the competition between the factors mentioned above the establishment of a spatially nonuniform texture with respect to **l** and **d** is more the rule rather than the exception. Analogously, in the B phase a spatially nonuniform texture with respect to **n** is usually established, because the walls of the vessel and the external magnetic field have an orienting effect on **n**. As far as the angle θ is concerned, its equilibrium value is determined by the requirement that the spin-orbital (dipole-dipole) energy be minimum: $\theta_0 = \arccos(-1/4) \approx 104°$.

In the experimental and theoretical studies of superfluid liquid ^{3}He performed during the last decade, a great deal of attention was devoted to the study of the diverse textures appearing in the A and B phases. A convenient method for studying these textures is NMR. When the spin degrees of freedom deviate from the equilibirum configuration, the spin-orbital interaction creates an additional coherent rotating moment, which acts on the nuclear magnetic moments of ^{3}He and causes a shift in the transverse-NMR freqeuncy relative to the Larmor frequency $\omega_0 = \gamma H$, observed in the normal phase of liquid ^{3}He.[9]

It is clear that the nature of the NMR spectrum of superfluid ^{3}He must depend strongly on the equilibrium texture, which forms the background for the oscillations of the spin degrees of freedom. For example, in the case of the uniform equilibrium distribution of **l** and **d** in the A phase the transverse-NMR frequency is given by the formula

$$\omega_{tr} = \sqrt{\omega_0^2 + \Omega_A^2\cos 2\alpha}, \quad (10)$$

where $\Omega_A(T)$ is the dipole frequency associated with the above-mentioned coherent rotating moment, and α is the equilibrium angle between **d** and **l** (under the conditions created by the combined effect of the vessel walls and of an external magnetic field, the angle α can differ from zero (from π). A more complicated situation is realized in the presence of soliton textures (domain walls), within which the mutual orientation of the vectors **d** and **l** changes gradually,

over a characteristic dipole length of $\xi_D \approx 10^{-3}$ cm, from the configuration with $\mathbf{d}\|\mathbf{l}$ to the configuration with $\mathbf{d}\|-\mathbf{l}$. Within these textures, localized oscillatory modes of the magnetization, observed in the form of satellites in the NMR spectra of superfluid ^{3}He-A1, are formed.[10]

In the rotating state, superfluid phases of liquid ^{3}He should exhibit a number of peculiar new properties, because the restrictions imposed by the internal symmetry of the order parameter (by the topological structure of the degeneracy space) on the capability of undergoing local vortical motions can lead to the establishment of a very peculiar rotational state of the superlfuid component. An example of this is ^{4}He-II for which these restrictions are so stringent ($\nabla\times\mathbf{v}_s = 0$ everywhere except, possibly, along special lines) that the equilibrum rotation of the superfluid component is realized only because of the presence of a system of singular quantized Onsager-Feynman vortices.

The order-parameter space of the superfluid A phase of liquid ^{3}He is multidimensional [see Eq. (7)] and, for this reason, the topological restrictions, which we mentioned above, are less onerous. Indeed, the superfluid velocity in ^{3}He-A, as we saw, does not reduce to a gradient of a scalar [see (6)] and its curl, with an appropriately "arranged" texture of the orbital vector l, can be continuously distributed over the volume of the liquid.[11] Because of this, the circulation of the superfluid velocity $\mathbf{v}_s$ along some closed contour C.

$$\Gamma = \oint_C \mathbf{v}_s\, d\lambda = \int\int_\Sigma (\nabla\times\mathbf{v}_s)\, d\sigma \tag{11}$$

can assume a continuous series of values depending on the nature of the distribution of the l field over the surface Σ, supported by the contour under study. This is what distinguishes the superfluid A phase of ^{3}He from ^{4}He-II, where the circulation Γ is unavoidably quantized (in units of $\hbar/m_4$).

From what was said above it is evident that due to the formation of a smooth, periodic, singularity-free terxture of the l field, the superfluid component of ^{3}He-A can rotate (on the average) as a rigid body without the formation of a lattice of singular vortices. An example of an isolated axisymmetrical texture without singularities is the state of the A phase with the following oribtal structure of the order parameter[12]:

$$\Delta_1 + i\Delta_2 = (\cos\beta\cdot\boldsymbol{\rho} + \sin\beta\cdot\mathbf{z} + i\boldsymbol{\varphi})\, e^{i\varphi}, \tag{12}$$

where $\boldsymbol{\rho}$, $\boldsymbol{\varphi}$, and $\mathbf{z}$ are the unit basis vectors of a cylindrical coordinate system, and $\beta(\rho)$ varies smoothly from zero at $\rho = 0$ to π at some distance from the texture axis (oriented along $\mathbf{z}$). It is easy to verify (using Eq. (6)) that the texture under study is characterized by the following superfluid-velocity distribution:

$$\mathbf{v}_s = \frac{\Gamma(\rho)\,\boldsymbol{\varphi}}{2\pi\rho}, \tag{13}$$

with the circulation $\Gamma(\rho) = (h/2m_3)\,[1 - cos\beta(\rho)]$, which along a closed contour, far from the z axis, is equal to two times the circulation quantum (in units of $\Gamma_0 = h/2m_3$) and smoothly approaches zero as the contour is contracted around the texture axis. A significant factor is that a texture of the type (12) can be continuously "squeezed out" of the uniform state of the A phase (its topological charge equals zero) and, for this reason, the energy of condensation is not lost when it is formed, as occurs with the formation of a singular vortex in ^{4}He-II.

It is now clear that rigid-body (on the average) rotation of the superfluid component in ^{3}He-A can be imitated by forming a periodic lattice of nonsingular textures of the type (12) by joining them along the boundaries of unit cells.[13] One such possibility is shown in Fig. 2. Along the boundary of each unit cell the orbital vector l points downwards, and it gradually rotates to the opposite orientation at the center of the cell. The circulation of the superfluid velocity around the boundary of each such cell is equal to two times the circulation quantum ($\Gamma_c + 2\Gamma_0$). It should be recalled that since the circulation Γ is not quantized in ^{3}He-A, it can vary smoothly as the contour of integration is deformed. The circulation has a quantized value $\Gamma = N\cdot 2\Gamma_0$, where N is the number of cells enclosed by this contour.

If the periodic texture of the type examined above is realized in a cylindrical vessel with radius R (the diagram in Fig. 2 refers to the cross section perpendicular to the axis of the cylinder), then a circulation $\Gamma = (\pi R^2/\Sigma_c)\cdot 2\Gamma_0$, where Σ_c is the area of the unit cell, is established along the inner surface of the vessel. In order that the pattern imitate rigid-body (on the average) rotation of the superfluid liquid, the expression presented for Γ must be equal to $2\pi R\cdot\Omega R$, i.e., in the rotating vessel the equilibrium density of the cells should be $n_c = 1/\Sigma_c = \Omega/\Gamma_0$. It is clear that when each cell "carries" ν circulation quanta, the density is equal to $n_c = 2\Omega/\nu\Gamma_0$.

The example presented above merely serves to illustrate how an equilibrium circulation of the superfluid velocity can be created in rotating ^{3}He-A without resorting to a lattice of singular vortices. On the other hand, the question of precisely which specific periodic structure of nonsingular vortex structures is realized with a given angular rotational velocity requires a detailed analysis based on energy considerations. Quantitative calculations have shown[14] that in the absence of an external magnetic field, the square lattice of nonsingular vortex textures, each unit cell of which carries four circulation quanta ($\nu = 4$), is energetically the most favorable lattice structure. A detailed analysis[15] has also shown that this structure is stable only for relatively low values of $\Omega < \Omega_1 \approx 30$ rad/s. For angular velocities exceeding Ω_1, a lattice consisting of singular vortex textures, without singularities in the velocity field $\mathbf{v}_s$, but with singular cores due to the singularities in the l field[16] (the internal structure of these cores was studied in Ref. 17), must become preferable. As Ω

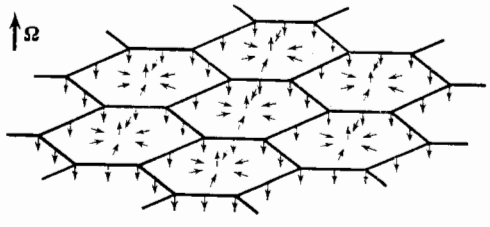

FIG. 2. Periodic texture of the l field of the rotating A phase (according to Volovik and Kopnin[13]).

is further increased, a loss of stability should also be expected in the lattice of singular vortex structures, described above, with a transition into the rotational state carrying the lattice of singular vortices with a unit quantum of circulation against the background of a uniform l field, perpendicular to the rotational axis.[15-18]

When an external magnetic field is switched on, the structure of the lattices formed by the vortex textures will be distorted due to the combined effect of magnetic anisotropy and spin-orbital interaction.[18] Since in equilibrium $\mathbf{d}\perp\mathbf{H}$, while the spin-orbital forces strive to maintain l oriented parallel to $\mathbf{d}$, the periodic l field of vortex textures must flatten out and as the intensity of the magnetic field is increased, the region where the vorticity of the superfluid velocity differs from zero will gradually contract toward the center of the unit cells, making room for regions where the field $\mathbf{l}\perp\mathbf{H}$ and is almost uniform. Thus, in the presence of a quite strong magnetic field, a soft core, within which $\nabla\times\mathbf{v}_s\neq 0$, forms around the axis of the nonsingular vortex texture. The radius of this nonsingular core in fields $H\gg H_c\approx 25\Gamma_c$ is determined by the dipole length $\xi_D\gg\xi$, at which, due to the spin-orbital interaction, a parallel orientation of l and $\mathbf{d}$, destroyed near the center of the vortex texture, is restored. It is clear that in the case of a lattice consisting of singular vortex structures, hard singular cores with dimensions ξ, within which the A phase is destroyed, are concentrated at the centers of soft cores.

We note that the lattice of singular vortex textures can be formed by splitting each nonsingular vortex texture with $\nu=2$ into two singular vortex textures with unit circulation quanta. To do so, a significant (topological) energy barrier, associated with the presence of hard cores in the singular vortex textures, must be overcome, but the final state obtained in the presence of a strong magnetic field turns out to be energetically more favorable.[18] Thus the lattice of nonsingular vortex textures in rotating ^{3}He-A must be metastable in fields $H\gg H_c$. On the other hand, it should be expected that it is easier to form it uniformly over the entire volume of the ^{3}He-A (by means of the above-mentioned "squeezing out" without the topological barrier) than it is to form the lattice of singular vortex textures, since the latter can apparently enter the bulk of the superfluid liquid only by being formed at the walls of the vessel.

Turning now to the proposed properties of the rotating B phase of ^{3}He it should be recalled [see Eq. (8)] that in this phase the superfluid flow is a potential flow, and for this reason the equilibrium state with the average value $\langle\nabla\times\mathbf{v}_s\rangle=2\boldsymbol{\Omega}$ can be realized only as a result of the formation of a lattice of singular vortices, similar to the well-studied picture in rotating ^{4}He-II. On the other hand, it should be expected that specific textural effects, arising due to the effect of counterflows of superfluid and normal components (with relative velocity $\mathbf{v}_s-\mathbf{v}_n$) on the orientation of the $\mathbf{n}$ axis (directrix), characterizing the B phase, will appear in rotating ^{3}He-B.

For $H\gg H_c$, the anisotropy energy density in the B phase, which depends on the orientation of $\mathbf{n}$ and is associated with the combined action of the magnetic field and superfluid counterflows, has the form[19]

$$F_{an}(\mathbf{n})=-a\left\{(\mathbf{nH})^2+\frac{2}{5}(\mathbf{u}\overleftrightarrow{R}(\mathbf{n})\mathbf{H})^2\right\}, \tag{14}$$

where $a\approx 10^{-12}$, $\mathbf{u}=(\mathbf{v}_s-\mathbf{v}_n)/v_c$ and v_c is the characteristic velocity with which the orienting action of the counterflows is comparable to the direct orienting effect of the applied magnetic field (it is easy to show that $v_c=\hbar/2m_3\xi_D=\Gamma_0/2\pi\xi_D\approx 0.1$ cm/sec near T_c). The first term in (14) describes the part of the dipole-dipole energy that arises due to the distortion of the completely isotropic state of the B phase in the presence of a magnetic field (as a result of the predominant breakdown of Cooper pairs with spin configuration $\uparrow\downarrow$). At the same time, due to the above-mentioned magnetic distortion ($\sim H^2$), the kinetic energy of the superfluid flow will also acquire an anisotropic correction, leading to the appearance of the second term in (14).

In the rotating vessel with ^{3}He-B the effect of counterflows of superfluid and normal components should be most distinctly manifested immediately after rotation is switched on, when the normal liquid is already entrained into rigid-body motion, while the superfluid component is still stationary (it may be conjectured that in order to form the equilibrium lattice of singular vortices, a macroscopic time will be required, analogously to the picture observed in ^{4}He-II). In this strongly nonequlibirum situation we have $\mathbf{u}=-(\boldsymbol{\Omega}\times\mathbf{r})/v_c$ and, if in an appreciable part of the volume of liquid $|\boldsymbol{\Omega}\times\mathbf{r}|\gg v_c$, then the counterflows must have a strong effect on the nature of the $\mathbf{n}$-field in the B phase. Subsequently, as the superfluid component is entrained into motion and the vortex structure is formed, the effect of the counterflows will weaken and, after an equilibrium state with $\langle\nabla\times\mathbf{v}_s\rangle=2\boldsymbol{\Omega}$ is established, the counterflows will be concentrated only in the regions between the vortices.

In order to describe the effect of the equilibrium vortex lattice on the orientation of the directrix $\mathbf{n}$ in the B phase, the second term in (14) must be averaged over a cross section perpendicular to the rotational axis $\mathbf{z}=\boldsymbol{\Omega}/\Omega$. As a result, we arrive at the following expression for the effective anisotropy energy of uniformly rotating ^{3}He-B[20]:

$$\langle F_{an}\rangle=-aH^2\left\{(\mathbf{nh})^2-\frac{2}{5}\lambda(\mathbf{z}\overleftrightarrow{R}(\mathbf{n})\mathbf{h})^2\right\}, \tag{15}$$

where $\mathbf{h}$ is a unit vector oriented parallel to the external magnetic field, while the dimensionless parameter $\lambda=\lambda(\Omega)$ characterizes the degree of the orienting effect of the superfluid flows flowing around the singular vortices and is given by the expression

$$\lambda=\left(\frac{\xi_D}{r_v}\right)^2\ln\frac{\sqrt{\pi}r_v}{\xi_c}, \tag{16}$$

where $\pi r_v^2=\Sigma_c=\Gamma_0/2\Omega$, and the cutoff radius ξ_c determines the effective size of the core of the vortex in the B phase.

Expression (16) for λ takes into account the contribution of vortex effects, due to the superfluid flows flowing past the vortices at a distance from their axes exceeding ξ_c. The region inside the cores (where the B phase is completely destroyed) can also contribute to the anisotropy energy of the rotating ^{3}He-B (this will be discussed in greater detail below).

By examining the case of an axial field ($\mathbf{H}\|\mathbf{z}$), it is easy to establish that

$$\langle F_{an}\rangle = aH^2[(1-\lambda)\sin^2\beta + \tfrac{5}{8}\lambda\sin^4\beta] + \text{const}, \quad (17)$$

and in equilibrium[20]

$$\sin^2\beta = \begin{cases} 0, & \lambda < 1, \\ \frac{4}{5}\left(1-\frac{1}{\lambda}\right), & \lambda > 1. \end{cases} \quad (18)$$

Thus, in a large volume of rotating ^{3}He-B (when the orienting effect of the vessel walls can be ignored), there exists a threshold value $\lambda = 1$, below which $\mathbf{n}\|\mathbf{H}$, as in the absence of rotation. At $\lambda = 1$, a phase transition occurs into the state with $\beta \neq 0$, which must be manifested as a shift in the frequency of the transverse NMR relative to the Larmor frequency ω_0 by an amount

$$\delta\omega_{tr} = \frac{\Omega_B^2}{2\omega_0}\sin^2\beta, \quad H \gg H_c, \quad (19)$$

where Ω_B is the dipole part of the longitudinal NMR of the B phase.

A different situation occurs if the magnetic field is inclined at some angle ϑ relative to the rotational axis. It can be shown[20] that in this case there is no threshold with respect to λ; in addition, for $\lambda \ll 1$

$$\sin^2\beta \approx 0.1\lambda^2\sin 2\vartheta, \quad (20)$$

and the effect of the vortex lattice on the orientation of the directrix $\mathbf{n}$ is maximum for $\vartheta = \pi/4$.

The characteristics of the behavior of rotating superfluid ^{3}He described above followed from the representations of the structure of A and B phases that were formulated over the last ten years, but until recently existed only in the imagination of theoreticians. The diversity of the expected new effects, as well as confidence in the fact that nature's inventiveness is limitless, increased interest in the experimental study of the problem of rotating ^{3}He.

3. THE ROTA ULTRA-LOW-TEMPERATURE ROTATING APPARATUS AND THE EXPERIMENTAL CELL

To realize the rotation of superfluid ^{3}He, a powerful ^{3}He–^{4}He dilution cryostat and an adiabatic demagnetization (Cu nuclei) cryostat, assembled on a massive platform "suspended" on a cushion of air (the air pressures was 4-6 bar) in order to decrease friction, were developed (Fig. 3). The rotation of the 360-kg unit is driven by a belt drive from an 18-W servomotor. The maximum angular rotational velocity attained is 2 rad/s. A measuring apparatus is mounted on the rotating platform connected by an electro-optical system to the computer that controls the experiment and stores the information collected. In order to decrease possible vibrations, which can lead to rapid warming up, special dampers were used and the entire apparatus was placed on an isolated, five-ton foundation. In addition, the dilution and adiabatic demagnetization cryostats were assembled to be as rigid as possible. As a result, the system was insensitive to both low- and high-frequency vibrations; with the flow of heat into the nuclear stage being equal to 30 mW and virtually independent of the rotational velocity.

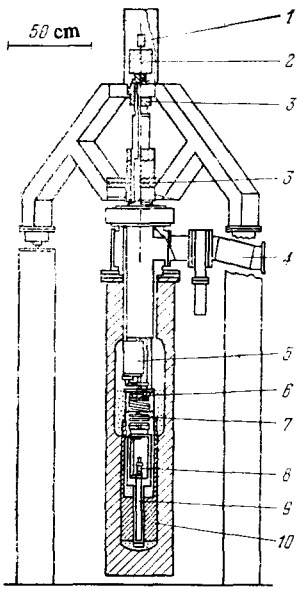

FIG. 3. Diagram of the ROTA ultra-low-temperature rotating apparatus. 1) Electro-optical data transmission line; 2) liquid-metal contacts for power input; 3) upper radial, lower radial and axial air bearings; 4) tube for evacuating the dilution cryostat (disconnected during rotation); 5) cryopump; 6) 1° K pot; 7) dilution cryostat; 8) experimental cell; 9) demagnetization stage; 10) superconducting solenoid (80 kOe).

The dilution cryostat use: three Frossati sintered heat exchangers,[21] whose total working area is equal to $\sim 100\,m^2$. During the process of cooling the nuclear stage, the dilution cryostat operates continuously. Then, after the adiabatic demagnetization is completed, the external pumping system is switched off and the ^{3}He is slowly pumped out of the cryostat with a cryosorption pump of novel design. The dilution cryostat operates autonomously for about 17 hours and the duration of the experiments in the rotational state is limited by the volume of ^{3}He in the dilution chamber.

The nuclear stage of the cryostat contains 30 mol of high-purity 0.5-mm copper wire. The dilution cryostat cools the nuclear stage to 20 mK in a magnetic field of 8 T. Then, by the method of adiabatic demagnetization of the Cu nuclei, a temperature of the order of 1 mK is attained. This is transferred through a conical contact to the sintered silver heat exchanger in the experimental cell. The conical contact is standardized to Soviet apparatus—an operating stationary nuclear demagnetization cryostat belonging to the Institute of Physical Problems of the USSR Academy of Sciences and an ultra-low-temperature rotating apparatus under construction at the Institute of Physics of the Academy of Sciences of the Georgian SSR, which makes it possible to interchange the experimental cells.

Since the characteristic properties of the rotating phases of liquid ^{3}He, described in the preceding section, are reflected in the nature of their textures, it was natural to use primarily NMR methods, which were so effective in probing the A and B phases in stationary vessels. The first experimental studies of the properties of ^{3}He-A and ^{3}He-B in the state of rotation were performed with the help of observations of the transverse-NMR spectra.

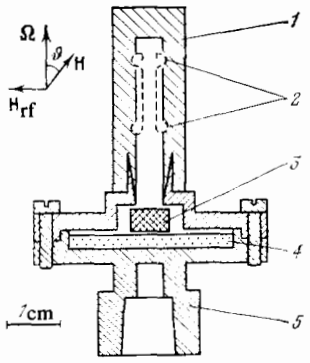

FIG. 4. Experimental ^{3}He cell. 1) Cell consisting of epoxy resin; 2) saddle-shaped NMR coils, 3) Pt NMR thermometer; 4) silver sintered heat exchanger; 5) conical contact.

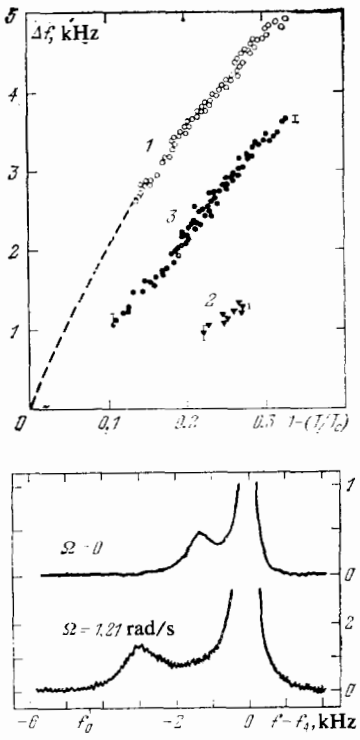

FIG. 5. Spectrum of the main absorption peak (1) and of the satellite lines: spontaneous line (2) and the line arising with rotation (3). The satellite lines are shown on the right (in units of the intensity of the main signal).

The experimental cell (Fig. 4) consisted of a cylindrical vessel 30 mm long with a diameter of 5 mm, whose axis is oriented along the rotation axis. The rf magnetic field was excited in saddle-shaped coils, wound around the generatrix of the cylinder. The constant magnetic field was created by two orthogonal solenoids, so that its orientation could be varied in a plane perpendicular to the poalrization of the rf field. The uniformity of the constant magnetic field was controlled by the correcting coils to within $\Delta H/H_0 \approx 4\cdot 10^{-5}$. The cell with ^{3}He, connected to the dilution cell so that its temperature was in the range 10–15 mK, was positioned next to the experimental cell. The NMR signal from this cell served as a reference point for calibrating the field. The magnetic field was scanned at a rate of the order of 1 G/min, while the 920-MHz NMR signal was stored in the memory of the computer and was recorded on an automatic plotter. Data from a PLM-3 platinum NMR thermometer, whose sensor was positioned at the bottom of the experimental cell, were recorded in phase with the scanning of the magnetic field. Most of the measurements were performed under conditions of natural heating-up of the sample at a rate of 1.5 μK/min; in addition, the rotation was usually turned on and off at intervals sufficient for establishing equilibrium, but in many cases the experiments were performed in a state of continuous rotation.

4. NMR SPECTROSCOPY OF ROTATING ^{3}He-A

The first information on the rotating A phase of liquid ^{3}He was extracted from the anlysis of the line shape of the transverse-NMR line. It turned out that as the angular velocity is increased, the absorption peak at a frequency of $\omega_{tr} \approx \omega_0 + (\Omega_A^2/2\omega_0)$ [see Eq. (10) for the case $\alpha = 0$ and $\omega_0 \gg \Omega_A$] "squats down" and is broadened with the integrated intensity remaining unchanged.[22] The proportionality of the observed effect to the angular velocity gave a basis for associating it with the formation of a system of vortices in the rotating A phase with an equlibrium density $n_c \sim \Omega$.

Further experiments,[23] performed with an improved resolution, revealed important details of the absorption spectrum of transverse NMR in rotating ^{3}He-A. It was found that the main peak is accompanied by a weak satellite at a frequency of $\omega_{sat} < \omega_{tr}$, virtually independent of the angular rotational velocity, while the intensity I_{sat} is proportional to Ω. Figure 5 shows a fragment of the data for the satellite mentioned.

It should be noted that in many cases, a second satellite, situated closer to the main absorption peak, was observed in the experiments. It appeared in the nonrotating vessel in the case of rapid passage into the A phase from the normal state of the liqud ^{3}He (see the left side of Fig. 5). An analysis of this secondary peak showed that it is associated with the formation of soliton textures, observed previously in stationary experiments.[24] In a cylindrical vessel, in the presence of an axial magnetic field, the appearance of so-called twist composite solitons should be expected. The oscillations of the magnetization, localized within the spin-orbital wells of the solitons, are observed precisely in the form of satellites in the transverse-NMR absorption spectra; in addition, the position of the above-mentioned secondary peak agrees very well with the theoretical prediction based onthe soliton model.[10] After the vessel with the ^{3}He-A is put into rotation, the intensity of the soliton satellite gradually decreases with time and approximately 30 min later the satellite vanishes completely.

Turning now to the newly observed satellite in the transverse-NMR spectrum of the rotating A phase, it should be emphasized that it has a large width and it has not been excluded that we are actually dealing with an unresolved structure arising as a result of superposition of close-lying peaks. If, however, it is interpreted as an isolated absorption peak, then the corresponding frequency can be represented

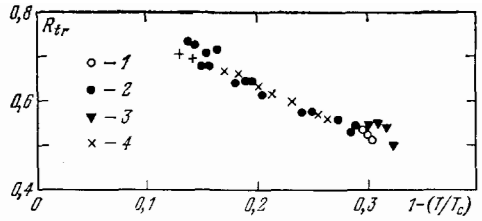

FIG. 6. Temperature dependence of R_{tr} for the vortex satellite for different angular velocities, Ω (rad/s) = 0.60 (1), 1.04 (2), 1.21 (3), and 1.43 (4).

in the standard form

$$\omega_{sat} = \sqrt{\omega_0^2 + R_{tr}^2 \Omega_A^2} \approx \omega_0 + R_{tr}^2 \frac{\Omega_A^2}{2\omega_0}, \quad (21)$$

where the renormalizing factor is $R_{tr}^2 < 1$. Figure 6 shows the experimental results for the temperature dependence of R_{tr}^2 for different angular rotational velocities. The fact that R_{tr}^2 and, therefore, the frequency of the satellite also, are virtually independent of Ω is interesting.

Figure 7 shows the experimental data on the dependence of the intensity of the new satellite on the angular rotational velocity, which can be described satisfactorily by the following empirical formula:

$$\frac{I_{sat}}{I_0} = 0.058\,\Omega, \quad (22)$$

where I_0 is the intensity of the main absorption peak at the frequency $\omega_{tr} \approx \omega_0 + (\Omega_A^2/2\omega_0)$, with the angular velocity expressed in rad/s.

An analysis of the results presented in Figs. 6 and 7 shows that the observed absorption peak is undoubtedly associated with the rotation of ^{3}He-A and is most likely formed within isolated vortex formations arising in the rotating vessel. This is indicated by the proportionality of the integrated intensity of the satellite to the angular velocity on the one hand and by the independence of its position from Ω on the other.

Further details on the characteristic properties of the transverse-NMR spectra in the rotating A phase of liquid ^{3}He can be found in Ref. 25, where, together with the questions mentioned above, data on the times of formation of the vortex satellite after the rotation is switched on as well as on the broadening of the main absorption peak in the rotational state are discussed.

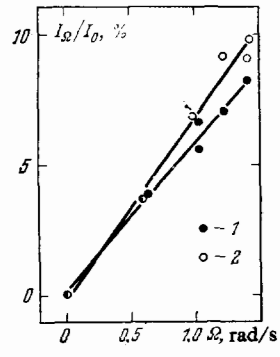

FIG. 7. Dependence of the relative intensity of the vortex satellite on the angular rotational velocity. 1) Rotation switched on in the state ^{3}He-A; 2) transition into the A phase occurring in the state of rotation.

In order to interpret the experimental data obtained, it is necessary to make a quantitative comparison with theoretical calculations. The starting point here is the assumption that the appearance of the detached absorption peak (satellite) is associated with the formation of localized oscillations of the magnetization, trapped, due to the coherent spin-orbital interaction, by inhomogeneities of the l field (mentioned in Sec. 2) of the soft cores of the periodic vortex structure of the rotation ^{3}He-A. The two-dimensional potential well of the dipole core of the vortex contains at least one bound state, which is excited under the conditions of transverse NMR, manifesting itself as the satellite described above. For a quantitative analysis of the spectrum of frequencies of localized spin oscillations, it is necessary to consider the wave equation for the transverse magnetization

$$(-\xi_D^2 \nabla^2 + U(\mathbf{r}))\, S_+ = \varepsilon S_+, \quad (23)$$

where $U(\mathbf{r})$ is the dimensionless dipole potential of the core of the vortex structure, and $\varepsilon = (\omega^2 - \omega_0^2/\Omega_A^2$.

In performing specific calculations of the spectrum of localized oscillations of the magnetization, one must start from realistic models of the soft cores, forming around the axes of the vortex textures in the presence of a strong magnetic field ($H \gg H_c \approx 30$ G), when their size is of the order of the dipole length ξ_D.[18] In the most general case, the triad $\mathbf{\Delta}_1$, $\mathbf{\Delta}_2$, $\mathbf{l}$), describing the local orbital state of the A phase, can be parameterized with the help of the Euler angles (α, β, γ) as follows:

$$\mathbf{\Delta}_1 + i\,\mathbf{\Delta}_2 = (\mathbf{u}_1 + i\mathbf{u}_2)\, e^{i\gamma}, \quad (24)$$

where

$$\mathbf{u}_1 = (\cos\alpha\cdot\mathbf{x} - \sin\alpha\cdot\mathbf{y})\cos\beta + \sin\beta\cdot\mathbf{z},$$
$$\mathbf{u}_2 = \sin\alpha\cdot\mathbf{x} + \cos\alpha\cdot\mathbf{y}. \quad (25)$$

It is easy to verify that the orbital vector is

$$\mathbf{l} = \mathbf{u}_1 \times \mathbf{u}_2 = -(\cos\alpha\cdot\mathbf{x} - \sin\alpha\cdot\mathbf{y})\sin\beta + \cos\beta\cdot\mathbf{z}, \quad (26)$$

so that the texture is described by the local values of the azimuthal angle α and of the polar angle β.

Using Eq. (6) it is easy to show that the superfluid velocity is equal to

$$\mathbf{v}_s = \frac{\Gamma_0}{2\pi}(\nabla\gamma + \cos\beta\nabla\alpha), \quad (27)$$

which once again confirms the impossibility of reducing $\mathbf{v}_s$ to the gradient of a globally defined scalar. At the same time, Eq. (27) indicates an extremely important fact, which is the key to constructing analytically different nonsingular vortex structures. It is easy to see from (27) that in the region where $\cos\varphi = 1$ it is possible to construct a state with a regular behavior of $\mathbf{v}_s$, if the quantity $\alpha + \gamma$ does not have singularities. Analogously, in the region where $\cos\beta = -1$, the superfluid velocity will be regular, if $\alpha - \gamma$ is a nonsingular function.

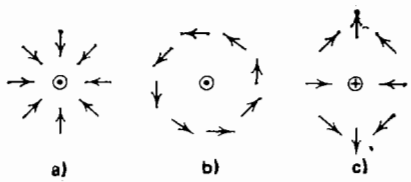

FIG. 8. Schematic illustration of the nonsingular radial (a), circular (b), and hyperbolic (c) vortex textures. The symbol ⊙(⊕) indicates the axis of the texture, where the vector **l** is oriented upwards (downwards).

Following the prescription formulated above, it is easy to construct several very simple isolated nonsingular vortex textures.

a) Mermin-Ho nonsingular radially-circular vortex texture

$$\left.\begin{aligned} &\alpha = -\varphi + \alpha_0, \quad 0 \leqslant \alpha_0 \leqslant \frac{\pi}{2}, \\ &\beta = \beta(\rho), \quad \beta(0) = 0, \quad \beta(\infty) = \frac{\pi}{2}, \\ &\gamma = \varphi, \quad \alpha + \gamma = \alpha_0 = \text{const}. \end{aligned}\right\} \tag{28}$$

This vortex is characterized by an axisymmetrical texture

$$\mathbf{l} = -(\cos\alpha_0 \cdot \boldsymbol{\rho} + \sin\alpha_0 \cdot \boldsymbol{\varphi})\sin\beta + \cos\beta \cdot \mathbf{z} \tag{29}$$

and by a regular distribution of the superfluid velocity

$$\mathbf{v}_s = \frac{\Gamma(\rho)\,\boldsymbol{\varphi}}{2\pi\rho} \tag{30}$$

with circulation $\Gamma(\rho) = \Gamma_0(1 - \cos\beta(\rho))$, in addition, $\Gamma(\infty) = \Gamma_0$. We note that with $\alpha_0 = 0$ we have a purely radial texture and with $\alpha_0 = \pi/2$ we have a purely circular texture.

b) Nonsingular cross-like (hyperbolic) vortex texture[26]:

$$\left.\begin{aligned} &\alpha = \varphi + \alpha_0, \quad 0 \leqslant \alpha_0 \leqslant \frac{\pi}{2}, \\ &\beta = \beta(\rho), \ \beta(0) = \pi, \quad \beta(\infty) = \frac{\pi}{2}, \\ &\gamma = \varphi, \quad \alpha - \gamma = \alpha_0 = \text{const}. \end{aligned}\right\} \tag{31}$$

This vortex is characterized by an axially unsymmetrical texture

$$\mathbf{l} = -[\cos(\alpha_0 + 2\varphi)\,\boldsymbol{\rho} - \sin(\alpha_0 + 2\varphi)\cdot\boldsymbol{\varphi}] \times \sin\beta + \cos\beta \cdot \mathbf{z} \tag{32}$$

and by a regular distribution of the superfluid velocity according to Eq. (30), but with the circulation $\Gamma(\rho) = \Gamma_0(1 + \cos\beta(\rho))$; in addition, once again, $\Gamma(\infty) = \Gamma_0$.

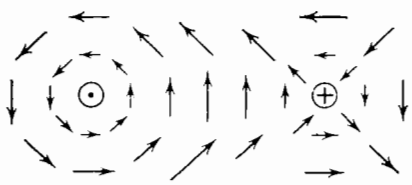

FIG. 9. Schematic illustration of the texture of the **l** field in the "molecule" of a circularly-hyperbolic vortex. With the transition from the axis of the circular texture to the axis of the hyperbolic texture, the vector **l** turns over smoothly into the opposite orientation.

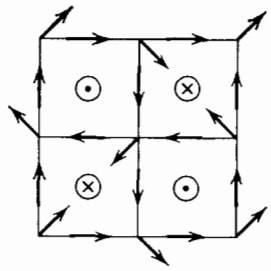

FIG. 10. Schematic illustration of the unit cell containing a pair of circularly-hyperbolic vortex textures. The circulation of the superfluid velocity along the boundary of the cell is equal to $4\Gamma_0$.

c) Nonsingular Anderson-Toulouse vortex texture:

$$\left.\begin{aligned} &\alpha = -\varphi, \\ &\beta = \beta(\rho), \quad \beta(0) = 0, \quad \beta(\infty) = \pi, \\ &\gamma = \varphi. \end{aligned}\right\} \tag{33}$$

This vortex, as alrady mentioned in Sec. 2, is characterized by an axisymemtrical texture [Eq. (12)] and by a regular distribution of the superfluid velocity [Eq. (13)]; in addition $\Gamma(\infty) = 2\Gamma_0$.

Figure 8 illustrates schematically the radial, circular, and hyperbolic textures.

It is easy to see that from the vortex textures of the type a) and b) it is possible to construct smooth periodic textures, free of singularities in the velocity field $\mathbf{v}_s$ and which imitate rigid-body (on the average) rotation of the A phase of liquid ^{3}He. The building blocks here are "molecules," consisting of pairs of circularly-hyperbolic vortex textures and capable of being easily inscribed in the uniform **l** field (Fig. 9). From these "molecules" it is possible to form a periodic structure with tetragonal symmetry, whose unit cell is illustrated in Fig. 10 and contains two circularly-hyperbolic "molecules." It is easy to show that the circulation of the superfluid velocity along the closed contour, running around the boundary of this cell, is equal to $4\Gamma_0$. The described periodic structure in rotating ^{3}He-A was first examined in Ref. 26, and it was demonstrated in Ref. 14 that in the absence of an external magnetic field it is energetically the most favorable nonsingular vortex texture with an equilibrium density of unit cells $n_c = \Omega/2\Gamma_0$, which ensures an on-the-average rigid-body rotation of ^{3}He-A.

In the absence of a magnetic field the size of the "molecules" examined above, which comprise the equilibrium vortex lattice of the type described, is determined by the angular rotational velocity and does not have an intrinsic characteristic size. When a strong magnetic field is aplied,the situation changes radically. As already noted in Sec. 2, for $H \gg H_c$, soft cores, whose size is of the order of the dipole length ξ_D, form around the axes of the analytic vortex textures. With moderate rotational velocities the size of the unit cell of the vortex lattice r_v, which is proportional to $1/\Omega$, is much greater than ξ_D, and for this reason the distribution of the **l** field will be almost uniform over a wide area within each cell, if the size of the circularly-hyperbolic "molecule" is compressed to a quantity of the order of ξ_D. Thus for $H \gg H_c$ it

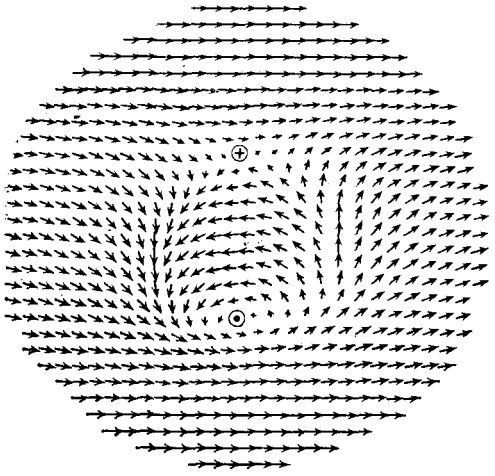

FIG. 11. Transverse cross section of the l field of the circularly-hyperbolic vortex "molecule" in the presence of a strong magnetic field (according to Seppala and Volovik[27]).

should be expected that the periodic vortex texture in rotating ^{3}He-A will be constructed from compact "molecules," which have a double quantum of circulation of the superfluid velocity and, most likely, will have a triangular symmetry, similar to the vortex lattices in superconductors and in ^{4}He-II.

An example of the compact "molecule" mentioned above is examined in Ref. 27 (Fig. 11), where the spectrum of localized spin oscillations, trapped within its dipolar potential well, was studied. According to the theoretical calculations, the previously introduced quantity R_{tr}, estimated for the texture illustrated in Fig. 11, is quantitatively close to the experimentally observed value.

The frequency of the satellite formed within the soft dipole core of a singular vortex texture in a field $H \gg H_c$ (a singular vortex, of course, also has a hard core within radius ξ) was also estimated in Ref. 27. Since, as it turned out, the dipole core of the singular texture is approximately two times smaller than the dipole core of a nonsingular vortex, the local vibrational level is located quite close to the upper edge of the potential well and R_{tr} is close to unity. A quantitative calculation showed that for the singular texture $R_{tr} \approx 0.98$ and the presence of such a weak isolated satellite [see Eq. (21)] could hardly be observed against the background formed by the broadened main peak. A theoretical estimate of the relative intensity of the vortex satellites also supports the fact that a system of analytic vortices with soft dipole cores was observed in rotating ^{3}He-A. It should be kept in mind, however, that according to calculations, performed in Refs. 18 and 27, in fields $H \gg H_c$ a lattice consisting of singular vortex textures may turn out to be energetically more favorable and for this reason it has not been excluded that the system of nonsingular vortices, observed expeirmentally, is metastable. this question requires further study.

5. NMR-SPECTROSCOPY OF ROTATING ^{3}He-B

Turning to the experimental data on NMR spectroscopy of the rotating B phase of liquid ^{3}He and their interpretation, it should be kept in mind, first of all, that in ^{3}He-B the magnetic length ξ_H^B, at which the parallel orientation of the directrix **n** and the field **H**, which was destroyed in some region of space, is restored, is determined by the competition between the very weak anisotropy energy $-aH^2(\mathbf{nh})^2$ and the gradient energy of the B phase and is estimated from the formula

$$\xi_H^B \approx \sqrt{\frac{a}{K}}\,\frac{1}{H}, \tag{34}$$

where K is the coefficient of rigidity of the order parameter of superfluid ^{3}He relative to spatial distortions of the condensate (details can be found in the review of Ref. 8). Because of the smallness of the coefficient a, the magnetic length ξ_H^B can have an entirely macroscopic value, comparable to the size of the vessel containing the ^{3}He-B, even in relatively strong fields $H \gg H_c$. For example, at $T = 0.7\ T_c$ and $H_0 = 284$ G the magnetic length $\xi_H^B \simeq 0.4$ mm, which is only six times smaller than the radius of the cylindrical vessel used in the experiments described below. This means that the presence of the vessel walls, which have an orienting effect on the directrix **n**, must be felt in a substantial part of the vessel volume, determining the nature of the equilibrium texture of the **n** field of the B phase.

In a magnetic field oriented along the axis of the stationary cylindrical vessel with ^{3}He-B, an axisymmetrical conically expanding (flare out) texture of the directrix is established. It is characterized by the fact that the vector **n** on the axis of the vessel is oriented parallel to **H** and as the distance from the center toward the periphery increases it becomes gradually tilted by an angle $\beta = \beta(\rho)$ from the axial orientation, reaching a tilt angle of $\beta(R) \simeq 63°$ relative to **H** at the walls of the vessel of radius R. At the same time the vector **n** is turned by an angle $\alpha = \alpha(\rho)$ relative to the radial direction, with $\alpha(R) \approx 60°$.

Oscillations of the magnetization, whose frequency spectrum can be studied by NMR methods, appear against the background formed by the equilibrium texture $\mathbf{n} = \mathbf{n}(\rho)$. If the texture is smooth enough (on the scale of the dipole length $\xi_D \ll \xi_H^B$), the NMR spectrum can be described in the first approximation by the model of local oscillators, assigning to each point with a fixed value of the angle β its "own" frequency.

$$\omega_{tr}(\rho) \approx \omega_0 + \frac{\Omega_B^2}{2\omega_0}\sin^2\beta, \tag{35}$$

and, in addition, knowing the distribution $\beta = \beta(\rho)$, the envelope of the spectral density can be constructed using the formula

$$P(\omega) = \frac{2}{R^2}\int \delta(\omega - \omega_{tr}(\rho))\,\rho\,d\rho. \tag{36}$$

In a more accurate approach, it is necessary to take into account the fact that due to the rigidity of the order parameter of the B phase the oscillations of the magnetization are collective modes and they must be described with the help of a wave equation of the type (23) with the dipole potential $U(\rho) = \sin^2\beta(\rho)$.

A detailed calculation of the texture of the **n** field of the B phase, confined in a cylindrical vessel and placed in an axial magnetic field, was performed in Ref. 28 for the case $\xi_H^B \ll R$ (see also Refs. 29 and 30). At a distance from the side

wall of the cylindrical vessel exceeding ξ_H^B, the tilt angle of the directrix away from the magnetic field is small and in the stationary case (i.e., in the absence of rotation) is described by the formula

$$\beta(\rho) \approx c \sqrt{\frac{2\pi R}{\xi_H}} e^{-R/\xi_H} I_1\left(\frac{\rho}{\xi_H}\right), \tag{37}$$

where $c \approx 1$, $\xi_H = (16/13)^{1/2} \xi_H^B$, and $I_1(x)$ is the modified Bessel function of the first kind.

From (37) it is easy to see that for $\rho \ll \xi_H$

$$\beta(\rho) \approx \beta_1\left(\frac{R}{\xi_H}\right)\frac{\rho}{\xi_H}, \quad \beta_1(x) = \frac{1}{2} c \sqrt{2\pi x} e^{-x}, \tag{38}$$

and, therefore, near the axis of the cylindrical vessel oscillations of the magnetization occur within a two-dimensional isotropic harmonic dipolar well

$$U(\rho) = \sin^2\beta(\rho) \approx \beta^2(\rho) \approx \beta_1^2 \left(\frac{R}{\xi_H}\right)\left(\frac{\rho}{\xi_H}\right)^2, \tag{39}$$

which leads to the formation of a spectrum of equidistant spin-wave levels, observed in the form of a series of transverse-NMR absorption peaks. Turning to Eq. (23) and using the oscillator potential (39), we can verify that the characteristic values of the quantity $\varepsilon = (\omega - \omega_0)/(\Omega_B^2/2\omega_0)$ are given by the formula $\varepsilon_n = (2n+1)\varepsilon_0$, where $\varepsilon_0 = 1.72(\xi_D/\xi_H)\beta_1(R/\xi_H)$. Thus the distance between the neighboring resonance peaks is equal to

$$\Delta\omega = 2\frac{\Omega_B^2}{2\omega_0}\varepsilon_0. \tag{40}$$

It should be kept in mind tht the harmonic-oscillator model is adequate only if the effective radius of localization of the spin-wave excitations satisfies $\rho_L < \xi_H \ll R$. Since $\rho_L^2 \approx \xi_D \xi_H/\beta_1$, the condition mentioned holds for $\beta_1 \xi_H > \xi_D$, i.e., if the magnetic length ξ_H is not too small.

From what was said above it follows that the effects of the vortices on the frequency spectrum of NMR in a rotating cylindrical vessel containing ^{3}He-B must be built up against the background formed by the pattern of equidistant absorption peaks described above. Turning to expression (17) for the density of the anisotropy energy, which takes into account the average orienting effect of superfluid vortex flows on the field of the directrix **n** of rotating ^{3}He-B, we verify that near the axis of the cylindrical vessel (where $\beta \ll 1$) $\langle F_{an}\rangle \simeq aH^2(1-\lambda)\beta^2$, while the effective magnetic length [see formula (34)] is

$$\xi_H^B(\lambda) = \sqrt{\frac{k}{a(1-\lambda)}}\frac{1}{H} = \frac{\xi_H^B(0)}{\sqrt{1-\lambda}}. \tag{41}$$

Thus, as the parameter $\lambda(\Omega)$, which characterizes the average effect of vortices on the orientation of the **n** axis, is increased, $\xi_H(\lambda)$ increases, which must lead to an increase of the slope of the dipole oscillator well [see formula (39)] and a corresponding increase of the distance $\Delta\omega(\lambda)$ between the neighboring absorption peaks inthe transverse-NMR spectrum of rotating ^{3}He-B.

Experimental studies of the frequency spectrum of NMR of the rotating B phase of liquid ^{3}He were performed in the cylindrical vessel used for NMR spectrosocpy of the rotating A phase (see Fig. 4). The very first measurements performed in the presence of an axial magnetic field ($H = 284$ G) with a pressure of $P = 29.3$ bar, led to the discovery of unexpected effects.[31] Figure 12 shows the spectrum of the transvwerse-NMR signal for ^{3}He-B in a state of rest ($\Omega = 0$) and in the rotating state ($\Omega = 0.6$ rad/sec). The structure of the spectrum is characteristic for NMR of the B phase under conditions of a limited geometry, when the effect of the vessel walls destroys the uniformity of the **n** field, creating a dipolar potential well in which standing spin-waves with a discrete frequency spectrum are formed, as described above. Precisely this picture was observed in the stationary cylindrical vessel in the presence of an axial magnetic field (almost equidistant absorption peaks are clearly visible in Fig. 12).

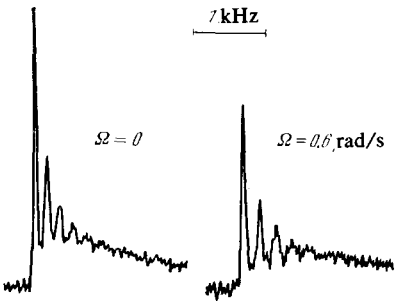

FIG. 12. Shape of the transverse-NMR signal for the B phase of ^{3}He in a magnetic field oriented along the axis of the cylindrical chamber.

Immediately after the rotation is switched on, for 1–2 minutes a transient state, during which the transverse-NMR spectrum described above is radically altered, was observed; in addition, judging from everything, the directrix **n** tilts strongly away from the axial direction. This picture corresponds to the nonequilibrium situation described in Sec. 2, when the superfluid part of the liquid is still not entrained into rotation and large counterflows of superfluid and normal components of ^{3}He-B exert a strong orienting action on the **n** field. The expected spectral density of the frequencies of the transverse NMR (more precisely, its envelope) is shown in Fig. 13 for different values of the angular velocities Ω. It is evident from this figure that due to the orienting effect of the nonequilibrium counterflows a distinct absorption peak is formed.[32] This conclusion qualitatively agrees with the observed transient effect.

After the end of the transient rotational regime the

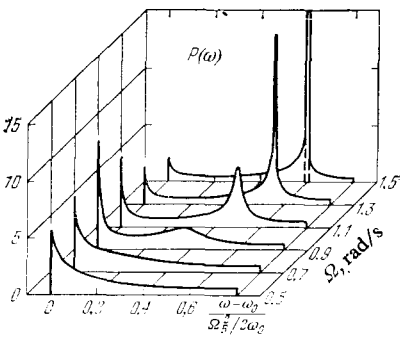

FIG. 13. Calculation of the envelope of the transverse-NMR absorption spectrum for the B phase in the presence of nonstationary counterflows of superfluid and normal components.

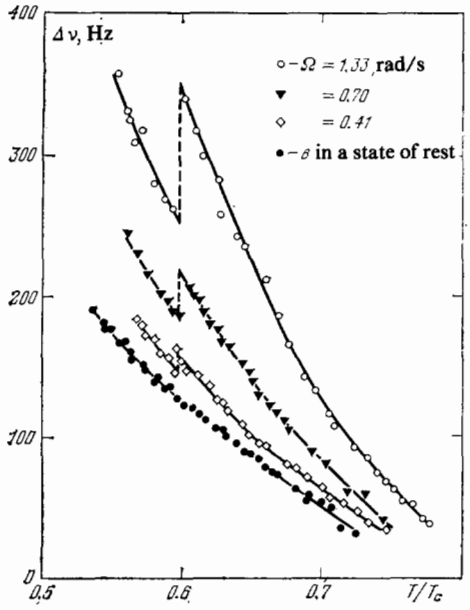

FIG. 14. Temperature dependence of the distance between neighboring transverse-NMR peaks for ^{3}He-B, placed in a cylindrical vessel rotating with an angular frequency Ω.

character of the NMR frequency spectrum of the B phase is restored (see the right side of Fig. 12), since the lattice of singular vortices formed prevents large counterflows of the superfluid and normal components, existing at the initial (nonequilibrium) stage of rotation of the ^{3}He-B. However, as ascertained in Ref. 31, the distance $\Delta\omega$ between the equidistant absorption peaks increases with the angular velocity (Fig. 14), which is undoubtedly associated with the average effect of the system of vortices, described above, on the texture of the **n** field of ^{3}He-B in the rotating cylindrical vessel.

The described behavior of the NMR spectrum of rotating ^{3}He-B completely corresponds to the formulated model of the superfluid B phase and does not contain any unexpected developments. On the other hand, the nature of the temperature dependence of $\Delta\omega$ with $\Omega \neq 0$, shown in Fig. 14, shows that at $T = 0.6\,T_c$ and $P = 29.3$ bar, we encounter an unexpected effect, which is manifested in the form of jumps in the magnitude of $\Delta\omega$. The lack of dependence of the temperature at which these jumps occur on the angular rotational velocity Ω (i.e., lack of dependence on the number of vortices) undoubtedly indicates that the observed phenomenon is associated with a jump-like change in the structure of separate vortices in the B phase of liquid ^{3}He.

Since the possible rearrangement of the structure of the singular vortex must primarily affect its core, we encounter for the first time a phenomenon occurring at a distance of the order of the coherence length ξ, which is the smallest scale in the hierarchy of characteristic lengths of superfluid ^{3}He-B. It is thus necessary to study the nature of the core structure of the vortex in the B phase and how its characteristics are manifested in the experimentally observed effects.

Because of the multicomponent nature of the order parameter of superfluid ^{3}He, the core of the vortex in the B phase can be set up by different methods, differing according to symmetry. It has not been excluded that one of the possible cores is filled with the superfluid phase, which is not realized in the bulk of the liquid ^{3}He. The jumps in the magnitude of $\Delta\omega$ observed; in Ref. 31 are associated with phase transitions within the core of the vortex, accompanied by a jump-like rearrangement of its structure.

The vortex cores make a definite contribution to the anisotropy energy (15) of the rotating ^{3}He-B. The parameter λ characterizes the averaged orienting effect of the vortices on the directrix **n**. In addition, the expression (16) describes the part that is due to the superfluid flows in the region $\rho > \xi_c$. The contribution of a vortex core (the region $\rho < \xi_c$) to λ is proportional to the area of its transverse cross section $\sigma_c = \pi\xi_c^2$. If it is assumed[28] that the vortex core is filled with the superfluid liquid with a magnetic-susceptibility anisotropy $\delta\chi_c$, then this contribution will be characterized by the parameter λ_c; in addition,

$$a\lambda_c = \frac{1}{2}\delta\chi_c \frac{\sigma_c}{\Sigma_c}, \tag{42}$$

while the total value $\lambda = \lambda_f + \lambda_c$, where λ_f is determined by the superfluid flows flowing around the vortices and is given by formula (16). As a result we arrive at the following model estimate of the paramter λ:

$$\lambda = n_c\left[\pi\xi_D^2 \ln\frac{\sqrt{\pi}r_v}{\xi_c} + \frac{1}{2}\frac{\delta\chi_c}{\Delta\chi_B}\left(\frac{\xi_D}{\xi}\right)^2\sigma_c\right]. \tag{43}$$

Near T_c the dipole length ξ_D does not depend on the temperature and is close to $0.6\cdot10^{-3}$ cm, and for $\Omega = 1$ rad/s, $\lambda_f \approx 0.1$. On the other hand, an estimate of the parameter λ, based on an anlysis of the experimental data for $\Delta\omega$, showed that for $\Omega = 1$ rad/s, $\lambda < 1$. This fact served as an argument[28] in support of the fact that $\lambda_c \gg \lambda_f$; in addition, in order to satisfy the requirement $\lambda_c \approx 1$, it was necessary to postulate a high anisotropy of the magnetic susceptibility of the vortex core ($\delta\chi_c \approx \Delta\chi_B$) and a large transverse core size ($\xi_c \approx 10\xi$). However, it should be kept in mind that the experimental data described above refer to temperatures far from T_c and, in addition, at $P = 30$ bar the dipole length is $\xi_D(0.5T_c) \approx 2\xi_D(T_c)$, i.e., $\lambda_f(0.5T_c) \approx 0.4\,\Omega$ [rad/sec], and the contribution of the core no longer apears to be predominant. We note, further, that λ_f increases as the pressure is decreased. Figure 15 shows the temperature dependence of λ_f for different pressures, constructed from estimates made in Ref. 33. As far as the value of λ_c is concerned, its estimation requires detailed information on the structure of the vortex core in the B phase.

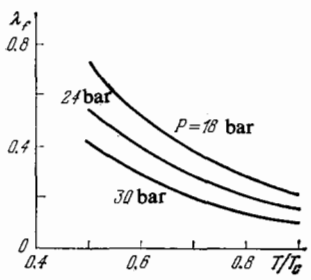

FIG. 15. Temperature dependence of the vortex parameter λ_f at different pressures.[33]

Before considering the question of the structural features of the vortex core in the B phase, we shall consider the methods used to determine the parameter λ experimentally. One of these methods is based on the analysis of the quantity $\Delta\omega$, which characterizes the distance between neighboring NMR absorption peaks in the rotating cylindrical vessel with ^{3}He-B. It was already pointed out that the average effect of vortices on the **n** field leads to a renormalization of the effective magnetic length [see formula (41)], which is manifested in the dependence of $\Delta\omega$ on λ. It was this renormalization that provided the first information on $\lambda = \lambda(\Omega, T)$ at $P = 29.3$ bar in an axial magnetic field.

Later it became clear that more reliable information on $\lambda = \lambda(\Omega, T, P)$ can be extracted from experiments performed in the presence of an inclined magnetic field, forming some angle ϑ with the rotational axis. In Sec. 2 it was already noted that according to Ref. 20, for $\vartheta \neq 0$, a shift should be observed in the transverse-NMR frequencies realtive to the Larmor frequency ω_0 by an amount

$$\delta\omega_{tr} \approx 0.1 \frac{\Omega_B^2}{2\omega_0} \lambda^2 \sin^2 2\vartheta. \tag{44}$$

This expression is valid for $\lambda \ll 1$ and shows that in this case the effect is maximum at a tilt angle $\vartheta = \pi/4$. For arbitrary values of the parameter λ, the shift in the NMR frequencies in the rotating B phase in the presence of an inclined field, is given by the equation[32]

$$\delta\omega_{tr} = \frac{4}{5} \frac{\Omega_B^2}{2\omega_0} (1-u), \tag{45}$$

and, in addition, the quantity $u = u(\pm, \vartheta)$ satisfies the equation

$$u\cos 2\vartheta + \left(u^2 - \frac{1}{2}\right)(1-u^2)^{-1/2} \sin 2\vartheta = \frac{1}{\lambda}. \tag{46}$$

It is easy to verify that the estimate (44) is reproduced for $\lambda \ll 1$, while in the general case the frequency shift is maximum for tilt angles $\vartheta_m = \vartheta_m(\lambda)$. Figure 16 shows the dependence of the normalized frequency shift on the parameter λ for different values of the angle ϑ.

In Refs. 34 and 35 the relation (45) was used as a source of information on the quantity $\lambda = \lambda(\Omega, T, P)$. Figure 17 shows the experimental data on the shift in the transverse-NMR frequency spectrum, observed in rotating ^{3}He-B ($\Omega = 1.4$ rad/s) for different tilt angles of the magnetic field relative to the axis of the cylinder. The frequency spectrum of th NMR signal, which is displaced relative to the absorption spectrum in the stationary B phase, is shown in the inset.

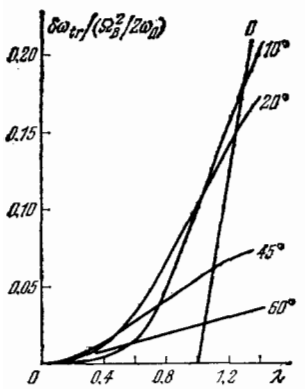

FIG. 16. Dependence of the normalized shift in the transverse-NMR frequency spectrum for the B phase, placed in a tilted magnetic field, on the vortex paramter λ (theory).

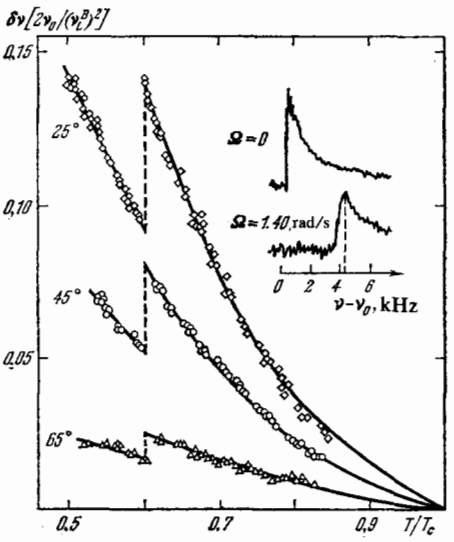

FIG. 17. Temperature dependence of the normalized shift in the transverse-NMR frequency spectrum for the B phase for different tilt angles θ of the magnetic field relative to the rotational axis. The absorption spectrum obtained at $T = 0.53\ T_c$ is shown in the inset.

It should be emphasized that the nature of the transverse-NMR spectrum in a tilted field differs appreciably from the absorption spectra observed in experiments with an axial magnetic field. As the angle ϑ is increased, the sharp left boundary of the spectrum in the stationary case ($\Omega = 0$) moves closer to the Larmor frequency ω_0 and an increasingly larger part of the spectral density is concentrated near its low-frequency boundary. This circumstance indicates that in the tilted field the equilibrium configuration of the **n** field differs in a significant way from the flare-out texture: in a large region of the transverse section of the cylindrical vessel the directrix of the B phase is oriented along the magnetic field. This fact can apparently be related to the special role of the surface energy in the cylindrical vessel, placed in a tilted magnetic field with $\vartheta > 14.5°$ (see below).

Returning to the large shift in the NMR frequency spectrum, due to the orienting effect of vortices on the directrix of the B phase under conditions of a tilted magnetic field (see Fig. 17), we once again observe the sharp breaks in the curves of the temperature dependence of the frequency shift $\sigma\omega_{tr}$ at $T = 0.6\ T_c$, reflecting the presence of a jump-like change in the parameter λ, stemming from the above-mentioned rearrangement of the internal structure of the vortex cores in ^{3}He-B. Relying on relations (45) and (46), it is possible to obtain from the experimental data (see Fig. 17) information on the coupling constant λ, describing the average interaction of vortices with the directrix **n**. The result of this analysis is shown in Fig. 18. At a pressure of $P = 29.3$ bar, the experimental points obtained with different tilt angles of the magnetic field do not exhibit an appreciable spread, which

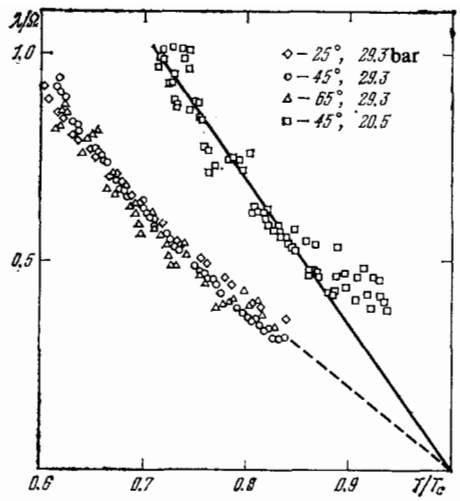

FIG. 18. Temperature dependence of the vortex parameter λ, measured for two values of the pressure with $\Omega = 1.40$ rad/s.

demonstrates the adequacy of the interpretation based on the theoretical results in Ref. 2. The same figure shows the temperature dependence of λ, measured at a pressure of $P = 20.5$ bar. The increase in the parameter λ as the pressure is decreased is clearly evident (compare with Fig. 15).

We shall now discuss briefly the nature of the equilibrium texture of the **n** field in the B phase, contained in the cylindrical vessel and placed in a tilted magnetic field. For $\vartheta \neq 0$ the boundary value of the angle β ($n_z = \cos\beta$) depends on the aximuth φ, which determines the position of the point on the circle along the inner surface of the cylinder. If the angle φ is measured from the plane defined by the vectors $\boldsymbol{\Omega}$ and **H**, then[32]

$$\sin\beta_s = -\frac{2}{\sqrt{5}}\sqrt{1 \pm \sin\vartheta\cos\varphi} \tag{47}$$

and the equilibrium texture in the volume of ^{3}He-B must be "inscribed" into this boundary condition. It is now clear that for tilt angles $\vartheta > 14.5°$, i.e., for $\sin\vartheta > 1/4$, both branches of the solution (47) must be used, in order to ensure that the boundary condition is satisfied along the entire inner surface of the cylindrical vessel. This discontinuous behavior of the angle β_s indicates the presence of a pair of linear surface singularities (so-called boojums) of the **n** field. For example, these linear defects can be situated along the generatrices of the cylinder with $\varphi = \pm\pi/2$. It is easy to verify that for $\vartheta < 14.5°$ the volume texture, which joins with the described surface configuration, is such that the orientation of the projection of the directrix **n** on the transverse plane differs little from the projection of the magnetic field almost everywhere. This is what explains the characteristic features of the NMR frequency spectrum in a tilted field and the large frequency shift observed in the case of rotation.

It should be kept in mind that the equilibrium texture described above in the tilted field is formed when ^{3}He enters the B phase in the presence of a fixed orientation of **H**. If, however, **H** is tilted away from the axis with an already formed flare-out texture, then the latter, in a somewhat distorted form, remains in the form of a metastable state (see Ref. 35 for a more detailed discussion).

Turning now to the question of the structure of the vortex core inthe B phase and the effects stemming directly from its characteristic features, it is necessary to start with a general analysis of the structure of the wave function of the condensate of triplet Cooper pairs with relative orbital angular momentum $L = 1$. A natural basis is the set of states $Y_{1m}(\mathbf{R})\chi_\mu$ with fixed projections of the orbital angular momentum $m = \pm 1, 0$ and total spin $\mu = \pm 1, 0$ on the corresponding quantization axes (the spherical harmonics Y_{1m} are functions of the "internal" spatial coordinate $\mathbf{R} = \mathbf{r}_1 - \mathbf{r}_2$ of the Cooper pair).

Any state of the superfluid condensate can be represented in the form of a superposition

$$\Psi(\mathbf{r}, \mathbf{R}) = \sum_{m\mu} a_{m\mu}(\mathbf{r})\, Y_{1m}(\mathbf{R})\, \chi_\mu, \tag{48}$$

and, in addition, in the nonuniform case the coefficients $a_{m\mu}$ depend on the coordinates of the center of mass $\mathbf{r} = (\mathbf{r}_1 + \mathbf{r}_2)/2$ of the Cooper pairs. We recall that for the A phase $m = \pm 1$, while $\mu = 0$ and, therefore, a_0 is the only nonvanishing coefficient. On the other hand, in the case of the B phase, in which the total angular momentum of the Cooper pairs is $J = 0$, the coefficients with $m + \mu = 0$, i.e., $\alpha_{1,-1}$, a_{00}, and $a_{-1,1}$, are nonvanishing.

Far from the core of the vortex with a unit quantum of circulation of the superfluid velocity, the state of the B phase is described by a triplet of coefficients (as above, (ρ, φ) are polar coordinates)

$$\left.\begin{aligned} a_{1,-1} &= c_{1,-1}(\rho)\, e^{i\varphi}, \\ a_{00} &= c_{00}(\rho)\, e^{i\varphi}, \\ a_{-1,1} &= c_{-1,1}(\rho)\, e^{i\varphi}, \end{aligned}\right\} \tag{49}$$

and, in addition, ignoring the effect of the magnetic field, the amplitudes $c_{m\mu}$ are equal to one another and at distances $\rho \gg \xi_c$ are virtually independent of ρ. As the center of the vortex is approached (in the region $\rho < \xi_c$) the amplitudes $c_{m\mu}(\rho)$ in (49) must gradually be suppressed, vanishing at $\rho = 0$. At the same time, within the core, new states with $m + \mu \neq 0$ can be mixed into the states already examined above, characterizing the B phase (if, of course, this lowers the energy of the system).

The structure of the vortex core in the B phase was studied theoretically in Ref. 36 taking into account states with $m + \mu = \pm 2$, i.e., the matrix $\hat{a}$ was selected in the form

$$\hat{a} = \begin{pmatrix} c_{1,1}e^{-i\varphi} & 0 & c_{1,-1}e^{i\varphi} \\ 0 & c_{00}e^{i\varphi} & 0 \\ c_{-1,1}e^{i\varphi} & 0 & c_{-1,-1}e^{3i\varphi} \end{pmatrix}, \tag{50}$$

and, in addition, the factors in front of the amplitudes c_{11} and $c_{-1,-1}$ were selected so that the energy density of the vortex state described by the matrix (50) would be independent of the azimuthal angle φ. The amplitudes $c_{m\mu}$ must be determined by minimizing the energy of the system (the sum of the energy of condensation and the gradient energy) under the condition

$$c_{m\mu}(0) = 0, \quad c_{11}(\infty) = c_{-1,-1}(\infty) = 0. \tag{51}$$

Figure 19 shows the results of the numerical calculations[36]

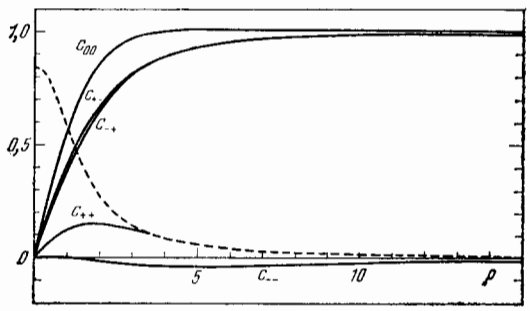

FIG. 19. Radial dependence of the coefficients $c_{m\mu}$ for the five-parameter vortex in the B phase.[36] The broken curve shows the energy density of the vortex.

of five amplitudes $c_{m\mu}(\rho)$, performed for the Ginzburg-Landau temperature range (near T_c). Of course, they refer only to the low-pressure B phase ($P < P_0$), when ^{3}He-B is directly adjacent to the normal phase of liquid ^{3}He. It is noteworthy that the so-called nonunitary state, characterized by the spontaneous magnetization

$$M(\mathbf{r}) \sim \sum_m [c_{m1}^2(\rho) - c_{m,-1}^2(\rho)], \tag{52}$$

is concentrated within the core of the vortex.

We note that vortices with magnetized cores can also exist, as demonstrated in Ref. 37, in superfluid Fermi systems with $^3P_2$ pairing (neutron stars).

The existence of vortices with magnetized cores in the rotating B phase of liquid ^{3}He was recently observed in Ref. 38. This gyromagnetic effect was revealed by comparing the NMR spectra obtained with rotational angular velocities Ω and $-\Omega$ (or for magnetic fields H and $-$H). As in the previously described experiments, two independent methods were used to observe the transverse-NMR frequency spectra: measurement of the distance $\Delta\omega$ between equidistant absorption peaks in the presence of an axial field and determination of the shift in the frequency spectrum $\delta\omega_{tr}$ in a tilted field ($\vartheta > 14.5°$). Figure 20 shows the data on the frequency shift $\delta\omega_{tr}$, measured with $P = 29.3$ bar, $\Omega = 1.4$ rad/s, and tilt angles of the magnetic field $\vartheta = 25°$ and $\vartheta = 155°$. The distinct gyromagnetic effect for $T < 0.6T_c$ shows that in the rotating B phase, a system of magnetic vortices with nonunitary cores is present in this region. An analysis of the data on $\Delta\omega$, measured with parallel and antiparallel orientations of Ω and H, leads to the same conclusion.

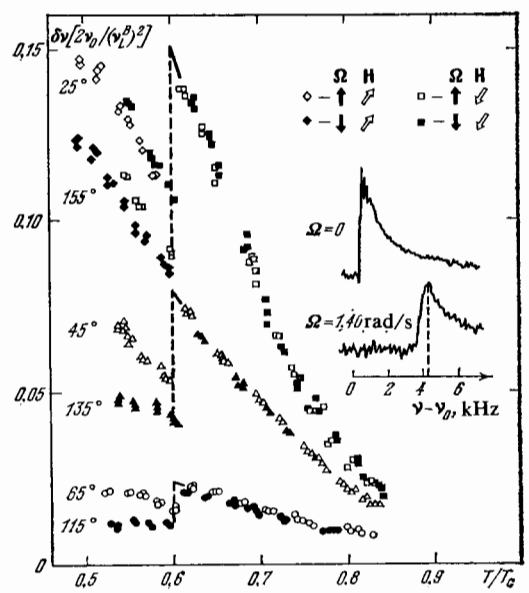

FIG. 20. The temperature dependence of the normalized shift in the transverse-NMR frequency spectrum of the B phase with $\Omega = 1.40$ rad/s in a tilted magnetic field. The symbols ○ and ● correspond to measurements with oppositely oriented rotations.

The effects described above indicate the presence of a gyromagnetic term which is linear with respect to Ω and H in the free energy of rotating ^{3}He-B

$$F_{gm} = \frac{4}{5} a\varkappa (\Omega \overleftrightarrow{R}(\mathbf{n})\,\mathbf{H})\,\Omega^{-1}, \tag{53}$$

which was proposed in Ref. 39 in order to describe phenomena related to the appearance of the orbital angular momentum L in the rotating B phase. It turned out that because the Cooper pairs in superfluid ^{3}He strongly overlap, the volume contribution of the effect mentioned to the constant $\varkappa$ is negligibly small and the magnetized vortex cores make the main contribution to it.[40] It is not difficult to obtain an estimate of the magnitude of the gyromagnetic constant. Since $a\varkappa \approx n_c M_c$, where M_c is the spontaneous magnetic moment of the core of a vortex of unit length ($M_c \sim \Gamma_0 \chi_n/\gamma$), the parameter is $\varkappa \approx (\chi_n/a\gamma)\Omega$.

Taking into account the gyromagnetic term described above, the anisotropy-energy density of the n field of the rotating B phase is given by the expression

$$\langle F_{an}\rangle = -aH^2\left\{(\mathbf{nh})^2 - \frac{2}{5}\lambda(\mathbf{z}\overleftrightarrow{R}(\mathbf{n})\,\mathbf{h})^2\right\} + \frac{4}{5}a\varkappa H(\mathbf{z}\overleftrightarrow{R}(\mathbf{n})\,\mathbf{h}), \tag{54}$$

the analysis of which shows that in a tilted magnetic field the shift in the frequecy of transverse NMR is described by the formula (45), where the quantity u is determined by the equation[39]

$$\lambda\left[u\cos 2\vartheta \pm \left(u^2 - \frac{1}{2}\right)(1-u^2)^{-1/2}\sin 2\vartheta\right] + \varkappa/H\left[\cos\vartheta \pm u(1-u^2)^{-1/2}\sin\vartheta\right] = 1. \tag{55}$$

The interpretation of the experimental data,[38] based on the relation (45), confirms the validity of the estimates of the gyromagnetic constant $\varkappa$ presented above. At the same time, the results of the measurements of the temperature dependence of $\delta\omega_{tr}$ (see fig. 20) show that the gyromagnetic effect is very distinct in the region $T < 0.6\,T_c$, whereas for $T > 0.6\,T_c$ it is practically unnoticeable. This fact once again confirms that in the indicated temperature ranges the vortices in the B phase of liquid ^{3}He have substantially different characteristics and, in addition, the difference is undoubtedly associated with the jump-like rearrangement of the structure of their cores at $T = 0.6\,T_c$ (we recall that this point refers to the pressure $P = 29.3$ bar).

The transition temperature T_t depends on the pressure.

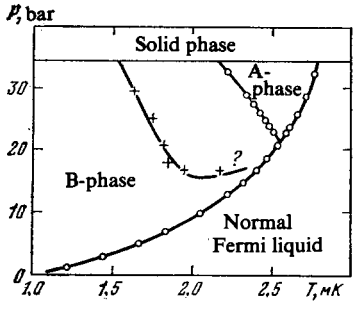

FIG. 21. Phase diagram of the vortex states in ^{3}He-B (schematically). There are no reliable experimental data in the immediate vicinity of T_c.

Figure 21 shows the phase diagram, reflecting the presently available information on the dependent $T_t = T_t(P)$. At low pressures the curve of the vortex phase transformation approaches T_c, but, near the transition into the normal phase, the accurancy of the measurements drops (in view of the weakening of the coherent dipolar effects, determining the nature of the NMR spectra), and for the time being there are no reliable data on the behavior of the curve $T_t = T_t(P)$ in the immediate vicinity of T_c.

Returning to the question of the possible structures of the vortex cores in the B phase, it should be kept in mind that the five-parameter solution studied in Ref. 36 describes the vortex state with the highest symmetry. Together with it, other states with lower (broken) symmetry, which differ from (50) by the structure of the core, can be realized. An exhaustive classification of the possible vortex states in ^{3}He-B was recently made in Ref. 41; in addition, computer calculations established the quantitative characteristics of vortices with different symmetry (energy, magnitude of the spontaneous magnetic moment, coupling constants λ and $\varkappa$). It was shown that the experimentally observed jump-like structural transition in the rotating B phase can be interpreted as a transition between vortex states with different symmetry.

6. CONCLUSIONS

In this paper we reviewed the basic results of studies of the properties of the superfluid phases of liquid ^{3}He in a state of rotation. The experimental data were obtained with the unique Soviet-Finnish ROTA apparatus using the method of NMR spectroscopy. Experimental and theoretical studies revealed the characteristic features of the textures in the rotating A and B phases, and an analysis of their results yielded rich information on the properties of superfluid ^{3}He in the rotational state. It was confirmed that the A phase can undergo uniform rotation without the presence of singular vortices. The observed smooth texture, which carries a distributed vorticity $1/2\nabla\times\mathbf{v}_s$, leads to the formation of a separate absorption peak in the transverse-NMR spectrum. A study of the rotating B phase revealed a phase transition, associated with the jump-like rearrangement of the structure of the vortex cores. It was shown that in the low-temperature phase the cores of vortices in ^{3}He have a spontaneous magnetic moment, which is manifested as a gyromagnetic effect in the rotating B phase.

All experimental data on the enumerated properties of the rotating superfluid phases of liquid ^{3}He were obtained with the help of observations of the nature of the frequecy spectrum of transverse NMR. The application of other methods (oscillations of bodies immersed in the superfluid liquid, absorption of ultrasound, mobility of ions) will permit obtaining in the near future new information on the properties of the A and B phases of ^{3}He in a state of rotation.

In working on this review we made extensive use of information from discussions of the questions touched upon here with our colleagues G. E. Volovik, A. D. Gongadze, V. I. Mineev, T. Ohmi, M. Salomaa, A. Feter, and P. Hakonen, to whom we are sincerely grateful.

[1]E. L. Andronikashvili and Yu. G. Mamaladze, Rev. Mod. Phys. **38**, 567 (1966).
[2]E. J. Yarmchuk and R. E. Packard, J. Low Temp. Phys. **46**, 479 (1982).
[3]D. D. Osheroff, R. C. Richardson, and M. Lee, Phys. Rev. Lett. **28**, 885 (1972).
[4]P. J. Hakonen, O. T. Ikkala, S. T. Islander, T. K. Markkula, P. Roubeau, K. M. Saloheimo, D. I. Garibashvili, and T. S. Tsakadze, Cryogenics **23**, 241 (1983).
[5]L. P. Pitaevskiĭ, Zh. Eksp. Teor. Fiz. **37**, 1794 (1959) [Sov. Phys. JETP **10**, 1267 (1960)].
[6]A. J. Leggett, Rev. Mod. Phys. **47**, 331 (1975).
[7]P. Wolfle, Rept. Progr. Phys. **42**, 269 (1979).
[8]V. P. Mineev, Usp. Fiz. Nauk **139**, 303 (1983) [Sov. Phys. USP **26**, 160 (1983)].
[9]A. J. Leggett, Ann. Phys. **85**, 11 (1974).
[10]K. Maki and P. Kumar, Phys. Rev. B **17**, 1088 (1978).
[11]N. D. Mermin and T.-L. Ho, Phys. Rev. Lett. **36**, 594 (1976).
[12]P. W. Anderson and G. Toulouse, Phys. Rev. Lett. **38**, 508 (1977).
[13]G. E.Volovik and N. B. Kopnin, Pis'ma Zh. Eksp. Teor. Fiz. **25**, 26 (1977) [JETP Lett. **25**, 23 (1977)].
[14]T. Fujita, N. Nakahara, T. Ohmi, and T. Tsuneto, Progr. Theor. Phys. **60**, 671 (1978).
[15]A. L. Fetter, J. A. Sauls, and D. L.Stein, Preprint, Stanford; Princeton (1983).
[16]G. E. Volovik and V. P. Mineev, Zh. Eksp. Teor. Fiz. **72**, 2256 (1977) [Sov. Phys. JETP **45**, 1186 (1977)].
[17]P. Muzikar, J. Phys. (Paris) **39**, C6-53 (1978).
[18]G.E. Volovik and P. J. Hakonen, J. Low Temp. Phys. **42**, 503 (1981).
[19]W. F. Brinkman and M. C. Cross in: Progress in Low Tmperature Physics (1978), Vol. 7a, p. 105.
[20]A. D. Gongadze, G. E. Gurgenishvili, and G. A. Kharadze, Fiz. Nizk. Temp. **7**, 821 (1981) [Sov. J. Low Temp. Phys. 7, 397 (1981)].
[21]G. Frossatti, J. Phys. (Paris) **39**, C6-1578 (1978).
[22]P. J. Hakonen, O. T. Ikkala, S. T. Islander, O. V. Lounasmaa, T. K. Markkula, P. Roubeau, K. M. Saloheimo, G. E. Volovik, E. L. Andronikashvili, D. I. Garibashvili, and J. S. Tsakadze, Phys. Rev. Lett. **48**, 1838 (1982).
[23]P. J. Hakonon, O. T. Ikkala, and S. T. Islander, Phys. Rev. Lett. **49**, 1258 (982).
[24]C. M. Gould and D. M. Lett, Phys. Rev. Lett. **37**, 1223 (1976); *ibid.* **41**, 967 (1978).
[25]P. J. Hakonen, O. T. Ikkala, S. T. Islander, O. V. Lounasmaa, and G. E. Volovik, J. Low Temp. Phys. **53**, 423 (1983).
[26]T. L. Ho, Ph.D. Thesis, Cornell University (1978).
[27]H. K. Seppala and G. E. Volovik, J. Low Temp. Phys. **51**, 279 (1983).
[28]P. J. Hakonen and G. E. Volovik, J.Phys. C **15**, L1277 (1983).
[29]K. Maki and M. Nakahara, Phys. Rev. B **27**, 4181 (1983).
[30]K. W. Jacobsen and H. Smith, J. Low Temp. Phys. **52**, 527 (1983).
[31]O. T. Ikkala, G. E. Volovik, P. Yu. Khakonen, Yu. M. Bun'kov, S. T. Islander, and G. A. Kharadze, Pis'ma Zh. Eksp. Teor. Fiz. **35**, 338 (1982) [JETP Lett. **35**, 416 (1982)].
[32]G. E.Volovik, A. D.Gongadze, G. E. Gurgenishvili, M. M. Salomaa, and G. A. Kharadze, Pis'ma Zh. Eksp. Teor. Fiz. **36**, 404 (1982) [JETP Lett. **36**, 489 (1982)].
[33]S. Theodorakis and A. L. Fetter, J. Low Temp. Phys. **52**, 559 (1983).

[34]Yu. M. Bun'kov, M. Kruziuss, and P. Yu. Khakonen,Pis'ma Zh. Eksp. Teor. Fiz. **37**, 395 (1983) [JETP Lett. **37**, 468 (1983)].
[35]Yu. M. Bunkov, P. J. Hakonen, and M. Krusius in: Proc. of the Sanibel Symposium on Quantum Fluids and Solids, 1983, AIP Conf. Proc., No. 103, p. 194 (1983).
[36]T. Ohmi, T. Tsuneto, and T. Fjuita, Progr. Theor. Phys. **70**, 647 (1983).
[37]J. A. Sauls, D. L. Stein, and J. W. Serene, Phys. Rev. D **25**, 967 (1982).
[38]P. J. Hakonen, M. Krusius, M. M. Salomaa, J. T. Simola, Yu. M. Bunkov, V. P. Mineev, and G. E. Volovik, Phys. Rev. Lett. **51**, 1362 (1983).
[39]G. E. Volovik and V. P. Mineev, Pis'ma Zh. Eksp. Teor. Fiz. **37**, 103 (1983) [JETP Lett. **37**, 127 (1983)].
[40]G. E. Volovik and V. P. Mineev, Zh. Eksp. Teor. Fiz. **86**, 1667 (1984) [Sov. Phys. JETP **59**, No. 5 (1984)].
[41]G. E. Volovik and M. M. Salomaa, Phys. Rev. Lett. **51**, 2040 (1983).

Translated by M. E.Alferieff